

# IR physics from the holographic RG flow

Chanyong Park<sup>a\*</sup> and Jung Hun Lee<sup>b†</sup>

<sup>a</sup> *Department of Physics and Photon Science, Gwangju Institute of Science and Technology, Gwangju 61005, Korea*

<sup>b</sup> *College of General Education, Kookmin University, Seoul, 02707, Korea*

## ABSTRACT

Applying the holographic method, we investigate an RG flow and IR physics holographically when a two-dimensional conformal field theory is deformed by a relevant scalar operator. To do so, we first assume an RG flow from a UV to new IR CFT. On the dual gravity side, such an RG flow can be described by rolling down of a bulk scalar field from an unstable to stable equilibrium point. After considering a simple scalar potential allowing several local extrema, we study the change of a ground state along the RG flow. We show that the entanglement entropy at an IR fixed point leads to a logarithmic divergence due to restoring of the conformal symmetry. We study how the change of the ground state affects two-point functions. In the probe limit, we numerically calculate the change of a conformal dimension caused by the modification of the ground state. We further study the analytic form of the IR conformal dimension which is perfectly matched to the numerical result.

---

\*e-mail : cyong21@gist.ac.kr

†e-mail : junghun.lee@kookmin.ac.kr

# 1 Introduction

After the holography proposal, there were many attempts to understand various strongly interacting systems on the dual gravity theory side. The holographic relation or AdS/CFT correspondence is manifest for large supersymmetric theories like  $N = 4$  Super Yang-Mills theory and ABJM theory [1–7]. In these cases, IR physics is trivial because of the conformal symmetry. To investigate nontrivial IR physics holographically, one needs to break the conformal symmetry. In this work, we take into account a relevant deformation of conformal field theory (CFT) and investigate new macroscopic features at the IR fixed point by applying the holographic method.

The holography is one of the useful techniques to understand strongly interacting systems. Although the dual gravity theories of maximally supersymmetric gauge theories have been known, it still remains as an unresolved issue to find the dual gravity of non-supersymmetric theories appearing in nuclear and condensed matter physics. Nevertheless, if one can find the dual gravity theories of real physical systems, one get more information about new physics laws governing real systems. Since a relevant deformation breaks the conformal symmetry, it usually generates a nontrivial renormalization group (RG) flow and may allow a new IR CFT. In this case, the appearance of the IR CFT is due to the non-perturbative RG flow involving all quantum corrections. In the traditional quantum field theory (QFT), unfortunately, it is very difficult to figure out such a non-perturbative RG flow. However, one can investigate a non-perturbative RG flow by applying the holographic method [8–21].

Recently, quantum entanglement entropy has been widely studied in high energy physics as well as quantum information and condensed matter theory [22–34]. The entanglement entropy is one of the important quantities to characterize quantum correlation between subregions and plays a role of an order parameter in quantum phase transitions [35, 36]. It was well known that the entanglement entropy in the UV limit shows a universal feature proportional to the area of the entangling surface [37, 38]. For two-dimensional CFT, in particular, the entanglement entropy diverges logarithmically and the coefficient of the logarithmic divergence corresponds to the central charge of CFT. In the holography studies, it was proposed that the entanglement entropy can be described by the area of a minimal surface extending to the dual geometry [22, 23, 39]. It was also shown that the holographic method correctly reproduces the area law of the entanglement entropy in the UV limit. At a phase transition point in the IR region, another logarithmic divergence can occur due to the restoration of a conformal symmetry. This is also true at an IR fixed point. To see this, we consider a three-dimensional Einstein-scalar gravity theory which corresponds to a two-dimensional QFT flowing from a UV to IR CFT. On this background, we investigate the RG flow of the entanglement entropy which is crucially associated with the change of the ground state. We first numerically study the RG flow of the entanglement entropy and shows that the entanglement entropy diverges logarithmically at an IR fixed point. We also study the IR entanglement entropy analytically by using perturbation near the IR fixed point. We show how the entanglement entropy relies on the coupling constant along the RG flow and find that the entanglement entropy diverges at a critical coupling constant which is the value at the IR fixed point.

We further investigate the correlation function of a local operator when the ground state changes along the RG flow. According to the AdS/CFT correspondence, it was proposed that a geodesic length  $L(t, x_1; t, x_2)$  connecting two local operators at the boundary is related to the two-point function of the dual QFT [3, 40–50]

$$\langle O(t, x_1) O(t, x_2) \rangle \sim e^{-\Delta L(t, x_1; t, x_2)/R_{UV}}, \quad (1.1)$$

where  $\Delta$  means a conformal dimension of a local operator  $O(t, x_1)$ . This holographic prescription describes two-point functions of the dual QFT in the probe limit. The change of a ground state with the variation of coupling constants can affect two-point functions and modifies the conformal dimension at the IR fixed point which we call an anomalous dimension. We first investigate the conformal dimension near the fixed points analytically and then look into the variation of a conformal dimension numerically in the entire energy range. We show that the analytic prescription is perfectly matched to the numerical result.

The rest of this paper is organized as follows. In Sec. 2, we take into account a dual gravity theory which realizes the RG flow from a UV to IR fixed point. We investigate the change of the entanglement entropy along the RG flow which describes the modification of a ground state with varying a coupling constant. In Sec. 3, we study how the change of the ground state affects two-point functions and conformal dimensions in the probe limit. We conclude this work with some discussions in Sec. 4.

## 2 Holographic dual of the RG flow

Let us begin with briefly discussing universal features of two-dimensional QFT at critical points where the scale symmetry is restored [38, 51–53]. We take into account a transverse field Ising model whose Hamiltonian is given by

$$H_I = - \sum_{n=1}^{L-1} \sigma_n^x - g \sum_{n=1}^{L-1} \sigma_n^z \sigma_{n+1}^z, \quad (2.1)$$

where  $\sigma_n$  indicate the Pauli matrices at the site  $n$ . This model describes paramagnet with  $\langle \sigma_n^z \rangle = 0$  for  $g = 0$ , while ferromagnet with  $\langle \sigma_n^z \rangle = \pm 1$  appears as the ground state for  $g = \infty$ . Intriguingly, the transverse field Ising model allows a second-order quantum phase transition at  $g = 1$ . This feature becomes manifest when we study entanglement entropy. For  $g = \infty$ , since  $\langle \sigma_n^z \rangle$  allows two accessible configurations with opposite sign of magnetization, the resulting entanglement entropy is proportional to  $\log 2$ .

At the quantum phase transition point, the entanglement entropy shows a logarithmic divergence due to the scale symmetry. Applying the corner transfer matrix method, the entanglement entropy is given by [38]

$$\begin{aligned} S_E &= \epsilon \sum_{j=0}^{\infty} \frac{2j+1}{1+e^{(2j+1)\epsilon}} + \sum_{j=0}^{\infty} \log \left( 1 + e^{-(2j+1)\epsilon} \right) \quad \text{for } g < 1, \\ &= \epsilon \sum_{j=0}^{\infty} \frac{2j}{1+e^{2j\epsilon}} + \sum_{j=0}^{\infty} \log \left( 1 + e^{-2j\epsilon} \right) \quad \text{for } g > 1, \end{aligned} \quad (2.2)$$

where the energy gap between the energy levels is given by

$$\epsilon = \pi \frac{K(\sqrt{1-1/g^2})}{K(1/g)}, \quad (2.3)$$

and  $K(1/g)$  is a complete elliptic integral of the first kind. Near the critical point with  $g = 1$ , the entanglement entropy is reduced to

$$S_E \approx -\frac{1}{12} \log \left( 1 - \frac{1}{g} \right), \quad (2.4)$$

which shows a logarithmic divergence as  $g \rightarrow 1$ . A similar feature also occurs when a two-dimensional QFT flows into an IR fixed point where the restoration of the conformal symmetry makes the entanglement entropy diverge. Hereafter, we clarify this feature in the holographic setup.

We take into account a two-dimensional UV CFT deformed by a relevant operator. Even when a UV physics is weakly interacting, the IR physics after the RG flow can be strongly interacting. Therefore, knowing the correct IR physics requires understanding a nonperturbative RG flow. To do so, we consider a three-dimensional gravity theory with one bulk scalar field

$$S = \frac{1}{2\kappa^2} \int d^3 X \sqrt{-g} \left( \mathcal{R} - \frac{1}{2} \partial_M \phi \partial^M \phi - \frac{V(\phi)}{R_{UV}^2} \right). \quad (2.5)$$

To describe the RG flow from a UV CFT to a new IR CFT, we introduce the following simple scalar potential as a toy model

$$V(\phi) = 2R_{UV}^2 \Lambda_{UV} + \frac{M_\phi^2}{2} \phi^2 + \frac{\lambda}{4} \phi^4 = 2R_{UV}^2 \Lambda_{UV} + \frac{\lambda}{4} \phi^2 \left( \phi^2 - 2 \frac{m_\phi^2}{\lambda} \right), \quad (2.6)$$

where  $M_\phi^2 = -m_\phi^2 < 0$ ,  $\lambda > 0$  and  $\Lambda_{UV} = -1/R_{UV}^2$  with a UV AdS radius  $R_{UV}$ . Note that here we exploit dimensionless field  $\phi$  and coupling constants,  $m_\phi^2$  and  $\lambda$ . The scalar potential considered here allows one local maximum,  $V = -2\Lambda_{UV}$  at  $\phi = 0$ , and two degenerated local minima,  $V = 2R_{UV}^2 \Lambda_{UV} - m_\phi^4/4\lambda$  at  $\phi_\pm = \pm m_\phi/\sqrt{\lambda}$ .

We concentrate on the RG flow from a UV CFT to another IR CFT. Such an RG flow in the holographic setup can be realized by a geometric solution interpolating a local maximum to one of the local minima. A local maximum and minimum correspond to an unstable or stable equilibrium point respectively, so the scalar field rolls down from a maximum to minimum. In other words, a rolling motion in gravity maps to an RG flow of dual QFT. From now on, we focus on the RG flow from a UV CFT at  $\phi = 0$  to an IR CFT at  $\phi_+ = \phi_{IR}$ . To describe a relevant operator, we assume that the bulk field has a negative mass square in the range of  $0 < -M_\phi^2 = m_\phi^2 < 1$ . Assuming that the bulk field depends only on the radial coordinate, it does not break the boundary Lorentz symmetry. The most general metric ansatz preserving the boundary Lorentz symmetry is given by

$$ds^2 = dy^2 + e^{2A(y)} \eta_{\mu\nu} dx^\mu dx^\nu. \quad (2.7)$$

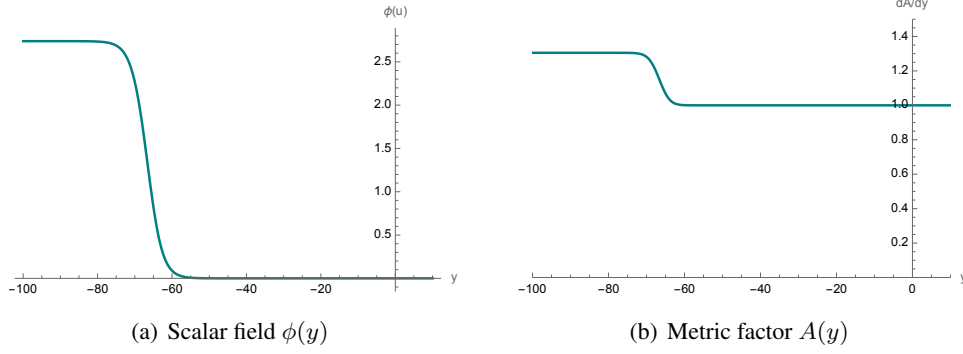


**Figure 1.** Profiles of (a) the scalar field  $\phi(y)$  and (b) metric factor  $A(y)$  where we take  $R_{UV} = 1$ ,  $m_\phi = \sqrt{3}/2$  and  $\lambda = 0.1$ . In this case, the deformation operator has a conformal dimension  $\Delta = 3/2$  and the IR fixed point occurs with  $\phi_{IR} = 2.7386$  and  $dA/dy = 1.3050$  at  $y = -\infty$ .

In this case, UV and IR fixed points appear at  $y = \infty$  and  $-\infty$ , respectively.

A geometric solution interpolating two fixed points of the RG flow is obtained by solving the equations of motion

$$0 = A'^2 - \frac{1}{4}\phi'^2 - \frac{m_\phi^2}{4R_{UV}^2}\phi^2 + \frac{\lambda}{8R_{UV}^2}\phi^4 - \frac{1}{R_{UV}^2}, \quad (2.8)$$

$$0 = A'' + A'^2 + \frac{1}{4}\phi'^2 - \frac{m_\phi^2}{4R_{UV}^2}\phi^2 + \frac{\lambda}{8R_{UV}^2}\phi^4 - \frac{1}{R_{UV}^2}, \quad (2.9)$$

$$0 = \phi'' + 2A'\phi' + \frac{m_\phi^2}{R_{UV}^2}\phi - \frac{\lambda}{R_{UV}^2}\phi^3, \quad (2.10)$$

where the prime means a derivative with respect to  $y$ . Here, the first equation is a constraint and the others determine dynamics of  $\phi$  and  $A$ . When we choose  $R_{UV} = 1$ ,  $m_\phi = \sqrt{3}/2$  and  $\lambda = 0.1$ , we depict a numerical solution in Fig. 1. The numerical results show that  $\phi$  and  $A'$  approach  $\phi_{IR} = 2.7386$  and  $A' = 1.3050$  at the IR fixed point ( $y \rightarrow -\infty$ ). Since a new AdS space appears at the IR fixed point,  $A' = 1.3050$  gives rise to an AdS radius  $R_{IR} = 0.7663$ .

Recalling that a  $(d + 1)$ -dimensional AdS space corresponds to the ground state of a  $d$ -dimensional CFT, the above interpolating solution maps to the ground state's RG flow where the coupling constant and degrees of freedom vary. Assuming that the boundary of bulk geometry is located at  $\bar{y}$ , the boundary position in the holographic study is identified with the RG scale of the dual QFT,  $\mu = e^{A(\bar{y})}$ . Moreover, the value of the scalar field at the boundary,  $\phi(\bar{y})$ , is reinterpreted as the coupling constant at the energy scale  $\mu$ . This prescription connects the geometrical interpolating solution to the RG flow in the momentum space. There is another holographic description for the RG flow. The entanglement entropy describing macroscopic quantum correlations is determined as a function of a subsystem size. In the RG flow of entanglement entropy, the RG scale is determined by a subsystem size rather than the boundary position. This resembles the real space RG flow widely used in condensed matter physics. Therefore, the entanglement entropy describes the real space

RG flow. As shown in the previous transverse field Ising model, the entanglement entropy can be used as an indicator for the quantum phase transition and fixed points.

Now, we investigate how the entanglement entropy modifies under the change of a ground state. To do so, we discuss the entanglement entropy near the fixed points analytically which may be useful to understand underlying theoretical structures of the RG flow. At the fixed points, the interpolation geometry is reduced to AdS spaces where the metric factor  $A(y)$  has to be linearly proportional to  $y$ . At the UV fixed point ( $y \rightarrow \infty$ ),  $A(y)$  is given by  $A(y) = y/R_{UV}$  with a UV AdS radius  $R_{UV}$ . Introducing a new UV coordinate

$$z = R_{UV} e^{-y/R_{UV}}, \quad (2.11)$$

the UV metric at  $z \rightarrow 0$  is rewritten as

$$ds_{UV}^2 = \frac{R_{UV}^2}{z^2} (-dt^2 + dx^2 + dz^2). \quad (2.12)$$

On the other hand,  $A(y)$  at the IR fixed point ( $y \rightarrow -\infty$ ) should be  $A(y) = y/R_{IR}$  where  $R_{IR}$  is an IR AdS radius. Introducing a new IR coordinate  $\bar{z}$  as

$$\bar{z} = R_{IR} e^{-y/R_{IR}}, \quad (2.13)$$

the IR metric for  $\bar{z} \rightarrow \infty$  becomes

$$ds_{IR}^2 = \frac{R_{IR}^2}{\bar{z}^2} (-d\bar{t}^2 + d\bar{x}^2 + d\bar{z}^2). \quad (2.14)$$

Comparing (2.11) and (2.13), the UV coordinates can be related to the IR ones

$$z = \frac{R_{UV}}{R_{IR}^{R_{IR}/R_{UV}}} \bar{z}^{R_{IR}/R_{UV}}, \quad dt = \frac{R_{IR}^{R_{UV}-R_{IR}}}{\bar{z}^{R_{UV}-R_{IR}}} d\bar{t} \quad \text{and} \quad dx = \frac{R_{IR}^{R_{UV}-R_{IR}}}{\bar{z}^{R_{UV}-R_{IR}}} d\bar{x}. \quad (2.15)$$

On the dual QFT point of view, the first relation describes the change of the RG scale. On the other hand, the last two relations describe the rescaling of the boundary coordinates along the RG flow.

Near the UV fixed point, since the bulk field rapidly suppresses in the asymptotic region ( $z \rightarrow 0$ ) for  $0 < m_\phi^2 < 1$ , it maps to a relevant operator. In this case, the effect of  $\lambda\phi^4$  is negligible. In the asymptotic region, more manifestly, the profile of  $\phi$  is approximately determined by

$$0 = \partial_z^2 \phi - \frac{1}{z} \partial_z \phi + \frac{m_\phi^2}{z^2} \phi. \quad (2.16)$$

The solution of this equation reads

$$\phi(z) = c_1 z^{2-\Delta_{UV}} + c_2 z^{\Delta_{UV}}, \quad (2.17)$$

where the conformal dimension of the dual operator  $O_\phi$  is given by

$$\Delta_{UV} = 1 + \sqrt{1 - m_\phi^2}. \quad (2.18)$$

For  $0 < m_\phi^2 < 1$ , the conformal dimension of the dual operator is in the range of  $1 < \Delta_{UV} < 2$ . This implies that the dual operator is relevant. Although the effect of a relevant deformation is negligible in the UV region, it significantly modifies IR physics due to nonperturbative quantum corrections. Near the UV fixed point, the RG scale is related to the radial coordinate,  $\mu \sim 1/z$ . Therefore,  $\phi(z)$  is reinterpreted as a coupling constant at the RG scale  $\mu$  on the dual QFT side. The  $\beta$ -function of the coupling constant becomes

$$\beta_\phi = \mu \frac{d\phi}{d\mu} = -(2 - \Delta_{UV})\phi + \dots, \quad (2.19)$$

which is consistent with the fact that the dual operator has a conformal dimension  $\Delta_{UV}$ .

A relevant operator usually causes a nontrivial RG flow and may lead to a new IR fixed point where the conformal symmetry is restored. Since an IR fixed point involving all quantum corrections is determined nonperturbatively, it is difficult to account for IR physics on the traditional QFT side. However, the holographic study can provide more information about IR physics. To see this, we take into account an IR limit at  $\bar{z} = \infty$  where the coupling constant is given by

$$\phi_{IR} = m_\phi / \sqrt{\lambda}. \quad (2.20)$$

Expanding the scalar field with a small fluctuation  $\delta\phi$

$$\phi = \phi_{IR} + \delta\phi, \quad (2.21)$$

the scalar potential is approximately near the IR fixed point

$$V \approx -2 \left( \frac{8\lambda + m_\phi^4}{8\lambda} \right) + m_\phi^2 \delta\phi^2, \quad (2.22)$$

where an IR cosmological constant is given by

$$2\Lambda_{IR} = -2 \left( \frac{8\lambda + m_\phi^4}{8\lambda} \right) \frac{1}{R_{UV}^2}. \quad (2.23)$$

Therefore, the IR AdS radius  $R_{IR}$  is related to the UV one

$$R_{IR} = \sqrt{\frac{8\lambda}{8\lambda + m_\phi^4}} R_{UV}. \quad (2.24)$$

Plugging the numerical values,  $R_{UV} = 1$ ,  $m_\phi = \sqrt{3}/2$  and  $\lambda = 0.1$ , we reproduce the numerical results obtained in Fig. 1,  $\phi_{IR} = 2.7386$  and  $R_{IR} = 0.7663$ . In this case, the deformation operator has a conformal dimension  $\Delta_{UV} = 3/2$  at the UV fixed point. Note that the IR AdS radius is always smaller than the UV one,  $R_{IR} < R_{UV}$ . Recalling that the central charges of two-dimensional CFTs at the fixed points are given by

$$c_{UV} = \frac{3R_{UV}}{2G} \quad \text{and} \quad c_{IR} = \frac{3R_{IR}}{2G}, \quad (2.25)$$

$R_{IR} < R_{UV}$  implies the  $c$ -theorem of two-dimensional QFTs,  $c_{UV} > c_{IR}$ .

Due to the restoration of the conformal symmetry at the IR fixed point, the dual geometry is again given by an AdS space in (2.14). To determine the  $\phi$ 's profile near the IR fixed point, we take into account the equation of motion for  $\delta\phi$

$$0 = \partial_{\bar{z}}^2 \delta\phi - \frac{1}{\bar{z}} \partial_{\bar{z}} \delta\phi - \frac{2 m_\phi^2 R_{IR}^2}{\bar{z}^2 R_{UV}^2} \delta\phi. \quad (2.26)$$

The solution of this equation reads

$$\delta\phi = d_1 \bar{z}^{2+\delta_{IR}} - d_2 \bar{z}^{-\delta_{IR}}, \quad (2.27)$$

where  $d_1$  and  $d_2$  are two integral constants and  $\delta_{IR}$  is given by

$$\delta_{IR} = \frac{\sqrt{8\lambda + m_\phi^4 + 16m_\phi^2\lambda}}{\sqrt{8\lambda + m_\phi^4}} - 1. \quad (2.28)$$

In this case, since  $\delta_{IR} > 0$ ,  $\delta\phi$  diverges as  $\bar{z} \rightarrow \infty$ . However, we assumed at the early stage that  $\phi$  has a finite value  $\phi_{IR}$  at the IR fixed point, so the first term in (2.27) must vanish. This implies that we should take  $d_1 = 0$ . Then, the resulting profile of  $\phi$  near the IR fixed point yields

$$\phi(\bar{z}) = \phi_{IR} - d_2 \bar{z}^{-\delta_{IR}} + \dots, \quad (2.29)$$

where  $d_2$  is given by a function of  $c_1$  and  $c_2$  in (2.17). Exploiting this scalar profile, we can determine the IR RG scale as a function of the coupling constant

$$\mu \sim \frac{1}{\bar{z}} \approx \left( \frac{\phi_{IR} - \phi(\bar{z})}{d_2} \right)^{1/\delta_{IR}}. \quad (2.30)$$

In addition, the  $\beta$ -function near the IR fixed point, where  $\mu \sim 1/\bar{z}$ , is given by

$$\beta_\phi = \mu \frac{d\phi}{d\mu} = -\delta_{IR} (\phi_{IR} - \phi(\bar{z})) + \dots. \quad (2.31)$$

At the IR fixed point with  $\phi(\bar{z}) = \phi_{IR}$ , the  $\beta$ -function automatically vanishes. This indicates the restoration of the conformal symmetry and that the dual operator becomes a marginal one with an IR conformal dimension,  $\Delta_{IR} = 2$ .

To further study the RG flow of the ground state, let us investigate the RG flow of the entanglement entropy. To describe the entanglement entropy valid in the entire energy scale, we calculate the entanglement entropy numerically. In the previous interpolation geometry (2.7), the entanglement entropy is governed by the area of a minimal surface [22, 23]

$$S_E = \frac{1}{4G} \int_{-\ell/2}^{\ell/2} dx \sqrt{y'^2 + e^{2A(y)}}, \quad (2.32)$$



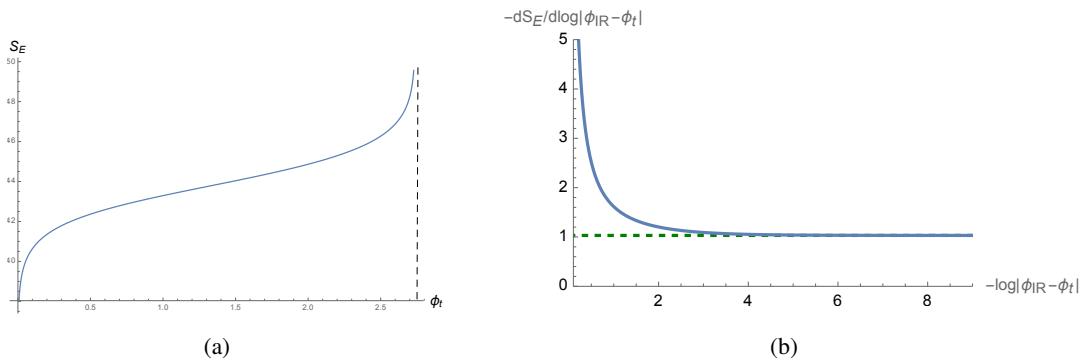


**Figure 2.** (a) Entanglement entropy depending on the coupling constant and (b) the coefficient of the IR entanglement entropy where we fix  $G = 1$ . (a) The entanglement entropy shows a logarithmic divergence at  $\phi_t \rightarrow \phi_{IR}$ . (b) When  $-\log(\phi_{IR} - \phi_t) \rightarrow \infty$  near the IR fixed point,  $-dS_E/d \log(\phi_{IR} - \phi_t)$  approaches 1.0316 which is consistent with the value expected by (2.45).

where the prime means a derivative with respect to  $x$ . Using the conserved quantity, the subsystem size and entanglement entropy are determined as functions of a turning point  $y_t$ , at which  $y' = 0$ ,

$$\ell = \int_{y_t}^{\Lambda_y} dy \frac{2}{e^{2A(y)} \sqrt{e^{-2A_t} - e^{-2A(y)}}}, \quad (2.33)$$

$$S_E = \frac{1}{2G} \int_{y_t}^{\Lambda_y} dy \frac{e^{-A_t}}{e^{2A(y)} \sqrt{e^{-2A_t} - e^{-2A(y)}}}, \quad (2.34)$$

where  $A_t = A(y_t)$  and  $\Lambda_y \rightarrow \infty$  denotes a UV cutoff. To perform these integrals numerically, we take  $G = 1$ ,  $R_{UV} = 1$ ,  $m_\phi = \sqrt{3}/2$ ,  $\lambda = 0.1$  and  $\Lambda_y = 20$ . Then, the entanglement entropy as a function of  $\phi(y_t) = \phi_t$  is depicted in Fig. 2(a). The numerical result shows that the entanglement entropy increases logarithmically at the UV fixed point ( $\phi_t = 0$ ), where we get rid of a UV divergence. At the IR fixed point ( $\phi_t = \phi_{IR} = 2.7386$ ), the entanglement entropy again diverges logarithmically. This implies that a logarithmic divergence of the entanglement entropy for two-dimensional QFT naturally appears when the scaling symmetry is restored. The numerical result in Fig. 2(b) shows that the coefficient of the logarithmic term approaches at the IR fixed point

$$-\frac{dS_E}{d \log(\phi_{IR} - \phi_t)} = 1.0316. \quad (2.35)$$

Although we calculated the entanglement entropy numerically, it is also important to know the analytic form for characterizing the parameter dependence. To do so, we reinvestigate the entanglement entropy analytically. Assuming that a subsystem has a small size  $\ell$  which is related to the inverse of an RG scale, a minimal surface in the UV limit extends to only the asymptotic region. Therefore, the dominant entanglement entropy in the UV region is governed by

$$S_E \approx \frac{R_{UV}}{4G} \int_{-\ell/2}^{\ell/2} dx \frac{\sqrt{z'^2 + 1}}{z}, \quad (2.36)$$

where  $z$  is the radial coordinate of the UV AdS geometry in (2.12). To evaluate the entanglement entropy, we introduce a turning point  $z_t$  at  $x = 0$ , where  $z' = 0$ . Then, the subsystem size and entanglement entropy in the UV limit ( $\ell \rightarrow 0$  and  $z_t \rightarrow 0$ ) are reexpressed in terms of the turning point

$$\ell(z_t) = \int_0^{z_t} dz \frac{2z}{\sqrt{z_t^2 - z^2}} = 2z_t + \dots, \quad (2.37)$$

$$S_E(z_t) = \frac{R_{UV}}{2G} \int_\epsilon^{z_t} dz \frac{z_t}{z\sqrt{z_t^2 - z^2}} = \frac{R_{UV}}{2G} \log \frac{z_t}{\epsilon} + \dots, \quad (2.38)$$

where  $\epsilon$  means a UV cutoff. Here, the ellipses mean higher order corrections caused by the deformation in the asymptotic region. The entanglement entropy relying on the subsystem size results in

$$S_E = \frac{c_{UV}}{3} \log \frac{\ell}{\epsilon} + \mathcal{O}(\ell). \quad (2.39)$$

In this case, the leading contribution comes from a two-dimensional UV CFT with small higher order corrections caused by the relevant deformation.

Recalling that the RG scale of the entanglement entropy is described by the subsystem size and that the subsystem size is determined by the turning point in (2.37), we can describe the RG scale of the entanglement entropy in terms of the turning point,  $\mu \sim 1/z_t$ . As a result, the value of  $\phi(z_t)$  at the turning point can be reinterpreted as the coupling constant at the RG scale  $\mu$ . In the UV region, the turning point  $z_t$  is reexpressed in terms of the coupling constant  $\phi(z_t) = \phi_t$

$$z_t \approx \left( \frac{\phi_t}{c_1} \right)^{1/(2-\Delta_{UV})}. \quad (2.40)$$

Then, the entanglement entropy becomes in terms of the coupling constant

$$S_E = \frac{c_{UV}}{3(2-\Delta_{UV})} \log \frac{\phi_t}{\phi_\epsilon} + \mathcal{O} \left( \phi_t^{1/(2-\Delta_{UV})} \right), \quad (2.41)$$

where  $\phi_\epsilon = \phi(\epsilon)$  means the coupling constant at the UV fixed point.

Let us study the entanglement entropy in a large subsystem size limit ( $\ell \rightarrow \infty$ ) which corresponds to the IR limit. The IR entanglement entropy in the holographic setup is defined as the integration over  $x$  in the range of  $-\ell/2 < x < \ell/2$ , so that it also contains the UV effect. Nevertheless, the leading contribution to the IR entanglement entropy comes from the minimal surface's area extending to the IR region. Therefore, the entanglement entropy near the IR fixed point is approximately given by

$$S_E \approx \lim_{\ell \rightarrow \infty} \frac{R_{IR}}{4G} \int_{-\ell/2}^{\ell/2} dx \frac{\sqrt{\bar{z}^2 + 1}}{\bar{z}}, \quad (2.42)$$

where  $\bar{z}$  is the radial coordinate of (2.14) in the IR region. Similar to the previous UV entanglement entropy, the leading subsystem size and IR entanglement entropy up to the UV divergence are determined by the turning point

$$\ell(\bar{z}_t) \approx \lim_{z_t \rightarrow \infty} 2\bar{z}_t, \quad (2.43)$$

$$S_E(\bar{z}_t) \approx \lim_{z_t \rightarrow \infty} \frac{R_{IR}}{2G} \log(\bar{z}_t) = \frac{c_{IR}}{3} \log(\bar{z}_t). \quad (2.44)$$

Therefore, the dominant IR entanglement entropy in terms of the coupling constant reads

$$S_E = -\frac{c_{UV} \sqrt{8\lambda}}{3 \left( \sqrt{8\lambda + m_\phi^4} + 16m_\phi^2\lambda - \sqrt{8\lambda + m_\phi^4} \right)} \log \left( \phi_{IR} - \bar{\phi}_t \right). \quad (2.45)$$

where  $\bar{\phi}_t = \phi(\bar{z}_t)$ . This shows that, similar to the previous transverse field Ising model, a logarithmic divergence appears at the IR fixed point due to restoration of the conformal symmetry. Using the numerical values used in Fig. 1, the coefficient of the logarithmic term results in

$$-\frac{dS_E}{d \log(\phi_{IR} - \phi_t)} = \frac{c_{UV} \sqrt{8\lambda}}{3 \left( \sqrt{8\lambda + m_\phi^4} + 16m_\phi^2\lambda - \sqrt{8\lambda + m_\phi^4} \right)} = 1.0316. \quad (2.46)$$

This is perfectly matched to the previous numerical result in (2.35).

### 3 Anomalous dimension of a local operator

Now, we investigate the RG scale dependence of correlation functions in order to understand another nonperturbative feature of the RG flow. To do so, we insert two local operators,  $O_\chi(t_1, x_1)$  and  $O_\chi(t_2, x_2)$ , into the ground state deformed by  $O_\phi$ . In the probe limit where the backreaction of  $O_\chi(t_i, x_i)$  with  $i = 1, 2$  is ignored, the background ground state, which is the dual of the previous gravity theory, is not modified. The holographic setup considered here describes how the change of the ground state affects two-point functions. Supposed that two scalar operators  $O_\chi$  have a conformal dimension  $\Delta_{UV}^\chi$  at the UV fixed point, then their two-point function is given by

$$\langle O_\chi(t_1, x_1) O_\chi(t_2, x_2) \rangle = \frac{1}{(-|t_1 - t_2|^2 + |x_1 - x_2|^2)^{\Delta_{UV}^\chi}}. \quad (3.1)$$

At the IR fixed point, the restoration of the conformal symmetry results in the same two-point function with a different IR conformal dimension. This is because, during the nontrivial RG flow, nonperturbative quantum effects crucially modify the conformal dimension. From now on, we discuss how to explain the change of the conformal dimension along the RG flow with the aid of holography.

In the holographic setup, we consider a bulk field  $\chi$  as the dual of  $O_\chi$ . To realize the conformal dimension  $\Delta_{UV}^\chi$ , we assume that  $\chi$  has mass  $-m_\chi^2/R_{UV}^2$  at the UV fixed point. In the asymptotic region, the bulk field  $\chi$  satisfies the following linear differential equation in the probe limit

$$\begin{aligned} 0 &= \frac{1}{\sqrt{-G}} \partial_M \left( \sqrt{-G} G^{MN} \partial_M \chi \right) + \frac{m_\chi^2}{R_{UV}^2} \chi \\ &= \frac{z^2}{R_{UV}^2} \left( \partial_z^2 \chi - \frac{1}{z} \partial_z \chi + \frac{m_\chi^2}{z^2} \chi \right). \end{aligned} \quad (3.2)$$

Assuming that the scalar field relies only on the radial coordinate, the mass of  $\chi$  determines the profile of  $\chi$  as

$$\chi = c_1 z^{2-\Delta_{UV}^\chi} + c_2 z^{\Delta_{UV}^\chi}, \quad (3.3)$$

where  $c_1$  and  $c_2$  are two integral constants and the dual operator  $O_\chi$  has a conformal dimension

$$\Delta_{UV}^\chi = 1 + \sqrt{1 - m_\chi^2}. \quad (3.4)$$

In this case, it is worth noting that, since  $\chi$  is governed by a linear second order differential equation,  $c_1$  and  $c_2$  are not mixed during the RG flow. Using the obtained UV conformal dimension, the two-point function of  $O_\chi$  at the UV fixed point results in

$$\langle O_\chi(t_1, x_1) O_\chi(t_2, x_2) \rangle = \frac{1}{(-|t_1 - t_2|^2 + |x_1 - x_2|^2)^{\Delta_{UV}^\chi}}. \quad (3.5)$$

Now, we take into account an IR correlation function. Since we consider the probe limit, the equation of  $\chi$  in (3.2) is still valid in the IR region although the background geometry deforms. Rewriting the equation (3.2) in terms of the IR coordinate  $\bar{z}$  by using (2.15), we obtain

$$0 = \partial_{\bar{z}}^2 \chi + \left(1 - \frac{2R_{IR}}{R_{UV}}\right) \frac{1}{\bar{z}} \partial_{\bar{z}} \chi + \frac{R_{IR}^2 m_\chi^2}{R_{UV}^2 \bar{z}^2} \chi \quad (3.6)$$

Solving this equation, the profile of  $\chi$  in the IR region reads

$$\chi = \bar{c}_1 \bar{z}^{2R_{IR}/R_{UV} - \Delta_{IR}^\chi} + \bar{c}_2 \bar{z}^{\Delta_{IR}^\chi}, \quad (3.7)$$

where the IR conformal dimension is given by

$$\Delta_{IR}^\chi = \frac{R_{IR}}{R_{UV}} \Delta_{UV}^\chi = \frac{\sqrt{8\lambda}}{\sqrt{8\lambda + m_\phi^4}} \left(1 + \sqrt{1 - m_\chi^2}\right). \quad (3.8)$$

Comparing the obtained IR solution with the UV solution in (3.3), the integral constants are determined as

$$\bar{c}_1 = \left(\frac{R_{UV}}{R_{IR}^{R_{IR}/R_{UV}}}\right)^{2 - \Delta_{UV}^\chi} c_1 \quad \text{and} \quad \bar{c}_2 = \left(\frac{R_{UV}}{R_{IR}^{R_{IR}/R_{UV}}}\right)^{\Delta_{UV}^\chi} c_2. \quad (3.9)$$

In the probe limit, the UV conformal dimension  $\Delta_{UV}^\chi$  flows into the IR one  $\Delta_{IR}^\chi$  along the RG flow because of the absence of mixing between  $c_1$  and  $c_2$ . Therefore, we expect that the following two-point function appears at the IR fixed point

$$\langle O_\chi(t_1, x_1) O_\chi(t_2, x_2) \rangle = \frac{1}{(-|t_1 - t_2|^2 + |x_1 - x_2|^2)^{\Delta_{IR}^\chi}}. \quad (3.10)$$

In this case, the anomalous dimension of  $O_\chi$  is given by

$$\gamma_\chi \equiv \Delta_{IR}^\chi - \Delta_{UV}^\chi = - \left(1 - \sqrt{\frac{8\lambda}{8\lambda + m_\phi^4}}\right) \Delta_{UV}^\chi < 0. \quad (3.11)$$

and the conformal dimension decreases along the RG flow,  $\Delta_{UV}^\chi > \Delta_{IR}^\chi$ .

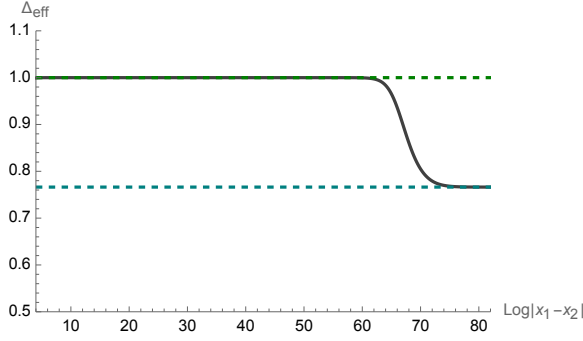


**Figure 3.** The RG flow of a conformal dimension of  $O_\chi$ . When the ground state is deformed by  $O_\phi$ , the change of the ground state affects on another operator  $O_\chi$ . Assuming that the UV conformal dimension is  $\Delta_{UV}^x = 1$ , the conformal dimension along the RG flow changes into  $\Delta_{IR}^x = 0.7663$  at the IR fixed point. This is consistent with the previous theoretical expectation in (3.8).

There is another holographic method calculating two-point functions in the probe limit. In the holographic setup, it was proposed that a two-point function can be described by a geodesic length  $L(t_1, x_1; t_2, x_2)$  connecting two local operators at the boundary [40–44, 48]

$$\langle O_\chi(t, x_1) O_\chi(t, x_2) \rangle \sim e^{-\Delta_{UV}^x L(t, x_1; t, x_2)/R_{UV}}, \quad (3.12)$$

where  $L(t, x_1; t, x_2)$  means a geodesic length. It is worth noting that the procedure calculating two-point correlations for three-dimensional gravity is similar to that used in the entanglement entropy calculation. This is because the minimal surface in the entanglement entropy calculation is reduced to a geodesic curve for three-dimensional gravity theory. However, this is not the case for higher dimensional gravity theories. Using this proposal, the known CFT's correlators at zero and finite temperature are reproduced [54–57].

Applying the holographic formula (3.12) to the previous interpolating geometry, the geodesic length is determined by

$$L(t, x_1; t, x_2) = \int_{y_t}^{\Lambda_y} dy \frac{2e^{-At}}{e^{2A(y)} \sqrt{e^{-2At} - e^{-2A(y)}}}. \quad (3.13)$$

When we take the UV conformal dimension of  $O_\chi$  to be  $\Delta_{UV}^x = 1$ , the RG flow of the conformal dimension of  $O_\chi$  for  $m_\phi = \sqrt{3}/2$  and  $\lambda = 0.1$  is plotted numerically in Fig. 3. The numerical simulation shows that the conformal dimension monotonically decreases from  $\Delta_{UV}^x = 1$  at the UV fixed point to  $\Delta_{IR}^x = 0.7663$  at the IR fixed point (see Fig. 3). This numerical IR conformal dimension can be understood by the previous analytic result

$$\frac{\Delta_{IR}^x}{\Delta_{UV}^x} = \frac{\sqrt{8\lambda}}{\sqrt{8\lambda + m_\phi^4}} = 0.7663. \quad (3.14)$$

In the probe limit, the analytic prediction in (3.8) is perfectly matched to the numerical result in Fig. 3.

## 4 Discussion

In the present work, we have studied the RG flow of a two-dimension QFT from a UV to IR fixed point by applying the holographic method. To describe such a RG flow, we took into account a relevant operator deforming UV CFT. On the dual gravity theory side, a UV fixed point corresponds to an unstable equilibrium point (or local maximum) with a negative potential energy at which an AdS space appears as a geometric solution. On the other hand, a new IR fixed point maps to a stable equilibrium point (or local minimum) where another AdS space becomes a geometric solution. To realize such a phenomenon, we consider a simple scalar potential, as a toy model, which allows local maximum and minima. Then, the RG flow from a UV to IR fixed point is reinterpreted as rolling down of a scalar field from an unstable to stable equilibrium point on the gravity theory side.

In general, a nonperturbative RG flow modifies the ground state of QFT, which also affects quantum correlation. Therefore, we expect that the entanglement entropy nontrivially changes along the RG flow. After introducing the holographic dual gravity realizing the RG flow from a UV to IR fixed point, we investigated the RG flow of entanglement entropy by applying the holographic formula. First, we numerically studied the change of entanglement entropy depending on the energy scale. Noting that the bulk scalar field can be mapped to a coupling constant on the dual QFT side, we also described the change of entanglement entropy in terms of the coupling constant. To understand the RG flow of entanglement entropy further, we also investigated the analytic behavior of the entanglement entropy near the fixed points. Using the perturbative expansion around the fixed points, we found the coupling constant dependence of the entanglement entropy near the UV and IR fixed points. We showed that the entanglement entropy of a two-dimensional QFT shows logarithmic behaviors at fixed points due to the restoration of the conformal symmetry. We explicitly showed that the analytic calculation near the fixed points are perfectly matched to the numerical result.

We further studied the RG flow of a conformal dimension in the holographic setup. To do so, we introduced two local operators and took into account the probe limit where two local operators do not modify the ground state. Even in this case, the change of the ground state affects the correlation function between two operators. In the holographic dual gravity, a two-point function in the probe limit can be described by a geodesic length connecting two local operators. Using this holographic method, we investigated the numerical RG flow of a two-point function when the ground state varies. To get more analytic information about the change of the conformal dimension, we also analytically studied the change of the two-point function near the fixed points. After introducing another bulk scalar field as the dual of local operators, we investigated its bulk equation of motion. From the solution of this equation, we looked into the analytic form of the IR conformal dimension, which is perfectly matched to the previous numerical result. These results show that the holographic dual gravity can explain the RG flow of the dual QFT correctly.

### Acknowledgement

C. P. was supported by Mid-career Researcher Program through the National Research Foundation of

Korea (NRF) grant funded by the Korea government (No. NRF-2019R1A2C1006639). J. H. L. was supported by the National Research Foundation of Korea (NRF) grant funded by the Korea government (No. NRF-2021R1C1C2008737)

## References

- [1] J. M. Maldacena, *Adv. Theor. Math. Phys.* **2**, 231 (1998), [arXiv:hep-th/9711200](#) .
- [2] J. M. Maldacena, *Phys. Rev. Lett.* **80**, 4859 (1998), [arXiv:hep-th/9803002](#) .
- [3] E. Witten, *Adv. Theor. Math. Phys.* **2**, 253 (1998), [arXiv:hep-th/9802150](#) [hep-th] .
- [4] E. Witten, *Adv. Theor. Math. Phys.* **2**, 505 (1998), [,89(1998)], [arXiv:hep-th/9803131](#) [hep-th] .
- [5] S. S. Gubser, I. R. Klebanov, and A. M. Polyakov, *Nucl. Phys. B* **636**, 99 (2002), [arXiv:hep-th/0204051](#) .
- [6] O. Aharony, O. Bergman, D. L. Jafferis, and J. Maldacena, *JHEP* **10**, 091 (2008), [arXiv:0806.1218](#) [hep-th] .
- [7] I. R. Klebanov and G. Torri, *Int. J. Mod. Phys. A* **25**, 332 (2010), [arXiv:0909.1580](#) [hep-th] .
- [8] J. de Boer, E. P. Verlinde, and H. L. Verlinde, *JHEP* **08**, 003 (2000), [arXiv:hep-th/9912012](#) .
- [9] M. Petrini and A. Zaffaroni, *PoS tmr99*, 053 (1999), [arXiv:hep-th/0002172](#) .
- [10] D. Z. Freedman, S. S. Gubser, K. Pilch, and N. P. Warner, *Adv. Theor. Math. Phys.* **3**, 363 (1999), [arXiv:hep-th/9904017](#) .
- [11] S. de Haro, S. N. Solodukhin, and K. Skenderis, *Commun. Math. Phys.* **217**, 595 (2001), [arXiv:hep-th/0002230](#) .
- [12] M. Bianchi, D. Z. Freedman, and K. Skenderis, *Nucl. Phys. B* **631**, 159 (2002), [arXiv:hep-th/0112119](#) .
- [13] R. C. Myers and A. Sinha, *JHEP* **01**, 125 (2011), [arXiv:1011.5819](#) [hep-th] .
- [14] H. Casini, M. Huerta, R. C. Myers, and A. Yale, *JHEP* **10**, 003 (2015), [arXiv:1506.06195](#) [hep-th] .
- [15] S. Gukov, *JHEP* **01**, 020 (2016), [arXiv:1503.01474](#) [hep-th] .
- [16] E. Kiritsis, F. Nitti, and L. Silva Pimenta, *Fortsch. Phys.* **65**, 1600120 (2017), [arXiv:1611.05493](#) [hep-th] .
- [17] J. K. Ghosh, E. Kiritsis, F. Nitti, and L. T. Witkowski, *JHEP* **05**, 034 (2018), [arXiv:1711.08462](#) [hep-th] .
- [18] C. Park, D. Ro, and J. Hun Lee, *JHEP* **11**, 165 (2018), [arXiv:1806.09072](#) [hep-th] .
- [19] U. Gürsoy, E. Kiritsis, F. Nitti, and L. Silva Pimenta, *JHEP* **10**, 173 (2018), [arXiv:1805.01769](#) [hep-th] .
- [20] J. K. Ghosh, E. Kiritsis, F. Nitti, and L. T. Witkowski, *JHEP* **02**, 055 (2019), [arXiv:1810.12318](#) [hep-th] .
- [21] C. Park and J. Hun Lee, *Phys. Rev. D* **101**, 086008 (2020), [arXiv:1910.05741](#) [hep-th] .
- [22] S. Ryu and T. Takayanagi, *Phys. Rev. Lett.* **96**, 181602 (2006), [arXiv:hep-th/0603001](#) [hep-th] .
- [23] S. Ryu and T. Takayanagi, *JHEP* **08**, 045 (2006), [arXiv:hep-th/0605073](#) [hep-th] .
- [24] I. R. Klebanov, D. Kutasov, and A. Murugan, *Nucl. Phys. B* **796**, 274 (2008), [arXiv:0709.2140](#) [hep-th] .
- [25] A. Karch, J. Maciejko, and T. Takayanagi, *Phys. Rev. D* **82**, 126003 (2010), [arXiv:1009.2991](#) [hep-th] .
- [26] T. Takayanagi, *Phys. Rev. Lett.* **107**, 101602 (2011), [arXiv:1105.5165](#) [hep-th] .
- [27] N. Ogawa, T. Takayanagi, and T. Ugajin, *JHEP* **01**, 125 (2012), [arXiv:1111.1023](#) [hep-th] .
- [28] J. Erdmenger, M. Flory, C. Hoyos, M.-N. Newrzella, and J. M. S. Wu, *Fortsch. Phys.* **64**, 109 (2016), [arXiv:1511.03666](#) [hep-th] .
- [29] J. Erdmenger, M. Flory, C. Hoyos, M.-N. Newrzella, A. O'Bannon, and J. Wu, *Fortsch. Phys.* **64**, 322 (2016), [arXiv:1511.09362](#) [hep-th] .
- [30] M. Rangamani and T. Takayanagi, *Holographic Entanglement Entropy*, Vol. 931 (Springer, 2017) [arXiv:1609.01287](#) [hep-th] .
- [31] T. Takayanagi and K. Umemoto, *Nature Phys.* **14**, 573 (2018), [arXiv:1708.09393](#) [hep-th] .
- [32] X. Jiang, P. Wang, H. Wu, and H. Yang, (2024), [arXiv:2406.09033](#) [hep-th] .
- [33] N. Jokela and J. G. Subils, *JHEP* **02**, 147 (2021), [arXiv:2010.09392](#) [hep-th] .
- [34] N. Jokela, H. Ruotsalainen, and J. G. Subils, *JHEP* **01**, 186 (2024), [arXiv:2310.11205](#) [hep-th] .

- [35] G. Vidal, J. I. Latorre, E. Rico, and A. Kitaev, *Phys. Rev. Lett.* **90**, 227902 (2003), [arXiv:quant-ph/0211074](#) .
- [36] M. Levin and X.-G. Wen, *Phys. Rev. Lett.* **96**, 110405 (2006), [arXiv:cond-mat/0510613](#) .
- [37] M. Srednicki, *Phys. Rev. Lett.* **71**, 666 (1993), [arXiv:hep-th/9303048](#) .
- [38] P. Calabrese and J. L. Cardy, *J. Stat. Mech.* **0406**, P06002 (2004), [arXiv:hep-th/0405152](#) .
- [39] H. Casini, M. Huerta, and R. C. Myers, *JHEP* **05**, 036 (2011), [arXiv:1102.0440 \[hep-th\]](#) .
- [40] L. Susskind and E. Witten, (1998), [arXiv:hep-th/9805114](#) .
- [41] S. N. Solodukhin, *Nucl. Phys. B* **539**, 403 (1999), [arXiv:hep-th/9806004](#) .
- [42] E. D'Hoker, D. Z. Freedman, and W. Skiba, *Phys. Rev. D* **59**, 045008 (1999), [arXiv:hep-th/9807098](#) .
- [43] H. Liu and A. A. Tseytlin, *Phys. Rev. D* **59**, 086002 (1999), [arXiv:hep-th/9807097](#) .
- [44] V. Balasubramanian and S. F. Ross, *Phys. Rev. D* **61**, 044007 (2000), [arXiv:hep-th/9906226](#) .
- [45] J. Louko, D. Marolf, and S. F. Ross, *Phys. Rev. D* **62**, 044041 (2000), [arXiv:hep-th/0002111](#) .
- [46] P. Kraus, H. Ooguri, and S. Shenker, *Phys. Rev. D* **67**, 124022 (2003), [arXiv:hep-th/0212277](#) .
- [47] L. Fidkowski, V. Hubeny, M. Kleban, and S. Shenker, *JHEP* **02**, 014 (2004), [arXiv:hep-th/0306170](#) .
- [48] C. Park and J. H. Lee, *JHEP* **02**, 135 (2021), [arXiv:2008.04507 \[hep-th\]](#) .
- [49] D. Rodriguez-Gomez and J. G. Russo, *JHEP* **06**, 048 (2021), [arXiv:2102.11891 \[hep-th\]](#) .
- [50] C. Park, (2024), [arXiv:2405.15108 \[hep-th\]](#) .
- [51] I. Peschel, M. Kaulke, and Ö. Legeza, *Annalen der Physik* **8** (1998).
- [52] K.-S. Kim, M. Park, J. Cho, and C. Park, *Phys. Rev. D* **96**, 086015 (2017), [arXiv:1610.07312 \[hep-th\]](#) .
- [53] P. Calabrese and J. L. Cardy, *Int. J. Quant. Inf.* **4**, 429 (2006), [arXiv:quant-ph/0505193](#) .
- [54] C. Park, *Eur. Phys. J. C* **81**, 521 (2021), [arXiv:2011.13555 \[hep-th\]](#) .
- [55] C. Park, *Phys. Lett. B* **842**, 137978 (2023), [arXiv:2209.07721 \[hep-th\]](#) .
- [56] C. Park, S.-J. Kim, and J. H. Lee, (2022), [arXiv:2212.01214 \[hep-th\]](#) .
- [57] H. Kim, J. Pal, and C. Park, (2023), [arXiv:2312.12669 \[hep-th\]](#) .